Optical Engineering 46(3), 033601 (March 2007)

Full-field strain measurement using a two-dimensional Savitzky-Golay digital differentiator in digital image correlation

Bing Pan
Huimin Xie
Zhiqing Guo
Tao Hua
Tsinghua University
Department of Engineering Mechanics
Beijing, China 100084
E-mail: xiehm@tsinghua.edu.cn

Abstract. Many published research works regarding digital image correlation (DIC) have been focused on the improvements of the accuracy of displacement estimation. However, the original displacement fields calculated at discrete locations using DIC are unavoidably contaminated by noises. If the strain fields are directly computed by differentiating the original displacement fields, the noises will be amplified even at a higher level, and the resulting strain fields are untrustworthy. Based on the principle of local least-square fitting using two-dimensional (2D) polynomials, a 2D Savitzky-Golay (SG) digital differentiator is deduced and used to calculate strain fields from the original displacement fields obtained by DIC. The calculation process can be easily implemented by convolving the SG digital differentiator with the estimated displacement fields. Both homogeneous and inhomogeneous deformation images are employed to verify the proposed technique. The calculated strain fields clearly demonstrate that the proposed technique is simple and effective. © *2007 Society of Photo-Optical Instrumentation Engineers.* [DOI: 10.1117/1.2714926]

Subject terms: digital image correlation; Newton-Raphson (N-R) method; Savitzky-Golay (SG); strain.

Paper 060201R received Mar. 20, 2006; revised manuscript received Jul. 23, 2006; accepted for publication Sep. 26, 2006; published online Mar. 29, 2007.

1 Introduction

Since it was originally established and advocated by a group of researchers at the University of South Carolina in 1982,[1] digital image correlation (DIC) has been improved by many scientific researchers and developed into an effective and popular full-field deformation measurement technique in experimental solid mechanics. A wide range of successful applications in scientific research and engineering have clearly demonstrated the versatility and effectiveness of this technique.

Among much published research literature with respect to DIC, it can be readily found that many research efforts have been devoted to improvement of the accuracy of displacement estimation, and different kinds of subpixel registration algorithms[2–9] have been developed. The main focus of this paper, however, is on the calculation of strain fields from the calculated displacement fields obtained by DIC. As in many tasks of experimental solid mechanics such as material mechanical testing and structure stress analysis, full-field strain distributions are more important and desirable.

It is obligatory to note that we can directly obtain displacements and displacement gradients (i.e., strains) using the Newton-Raphson (N-R) method[4,8,9] in DIC. However, just like any other measurement technique, the actual displacement fields of the tested object cannot be perfectly restored by the N-R method due to the unavoidable influences of various types of noises. The universally accepted displacement estimation accuracy of DIC is about ±0.02 pixel. Also, the error of estimated displacement gradients using the N-R method limits its use only to local strains greater than approximately 0.010. To obtain more reliable and accurate strain estimation, Sutton et al.[10] proposed a technique that involves smoothing the computed displacement fields with the penalty finite element method first and subsequently differentiating them to calculate strains. Since the noise level contained in the displacement field is significantly decreased after the smoothing operation, in consequence, this technique substantially increases the resolution in resulting strain estimations. However, smoothing noisy discrete data using the penalty finite element method is rather cumbersome both in mathematics deduction and in programming. Therefore, there remains a key problem in obtaining reliable and accurate full-field strain estimations from noisy displacement fields using a relatively simple yet effective technique.

In 1964, Savitzky and Golay[11] developed a digital filter to smooth and differentiate one-dimensional (1D) discrete data based on the principle of running least-squares polynomial fitting, which is generally called the Savitzky-Golay (SG) filter and is familiar to analytical chemists. The SG filter has acquired widespread applications in various scientific fields such as spectrology, digital signal processing, and digital image processing. In this paper, based on the simple idea of local least-square fitting with two-dimensional (2D) polynomials, we deduce a kind of 2D SG filter for calculating local strains from the displacement fields obtained by DIC. This is referred to as a 2D SG digital differentiator in this study, because it is an extension of the 1D SG digital differentiator.

The main objective of the study presented in this paper is to offer a simple and effective technique using a 2D SG digital differentiator to calculate full-field strain distributions from the original displacement fields obtained by DIC. In this paper, the principle of the N-R method is introduced in detail first. Then we describe the underlying principle of the 2D SG digital differentiator and give the filter coefficients. Also images of homogeneous and inhomogeneous deformation are employed to evaluate the proposed technique, and the calculation results clearly demonstrate the validity of the proposed technique.

2 Digital Image Correlation Using the Newton-Raphson Method

2.1 *Basic Principle of Digital Image Correlation*

In general, the DIC method is performed between two digital images of the test specimen surface acquired before and after deformation, which are referred to as the reference (or undeformed) image and the target (or deformed) image, respectively. It uses the random natural or artificial speckle patterns on the test specimen surface to obtain the full-field surface displacements by matching the interrogated subsets before and after deformation. Typically, a subset of $(2M+1)\times(2M+1)$ pixels from the reference image is chosen, and its corresponding location in the deformed image is determined. In practical implementation, a correlation function is predefined to evaluate the similarity between the reference subset and target subset. The matching procedure is completed through searching the peak position of the distribution of correlation coefficients. If the maximum or minimum (dependent on the correlation function used) correlation value is determined, the differences of the positions of the reference subset center and the target subset center yield the in-plane displacements u and v.

In order to achieve high spatial resolution of the displacement field, the calculation area in the reference image is generally divided into virtual grids. The displacement field is computed at each point of the virtual grids, and the distance between neighboring grids (i.e., grid step) is usually chosen between 2 and 10 pixels.

2.2 *Displacement Mapping*

Consider a 2D deformation of the interrogated subsets between the two images. As shown schematically in Fig. 1, a set of neighboring points in a reference subset is assumed to remain as neighboring points in the deformed (or target) subset. When the reference subset is small enough, we can assume that each of these points $Q(x,y)$ around subset center $P(x_0,y_0)$ in the reference subset is mapped to $Q'(x',y')$ in the target subset according to the following displacement mapping function:

$$x' = x_0 + \Delta x + u + \frac{\partial u}{\partial x}\Delta x + \frac{\partial u}{\partial y}\Delta y,$$

$$y' = y_0 + \Delta y + v + \frac{\partial v}{\partial x}\Delta x + \frac{\partial v}{\partial y}\Delta y, \tag{1}$$

where u,v are the displacement components for the subset center P in the x and y directions, respectively. The terms

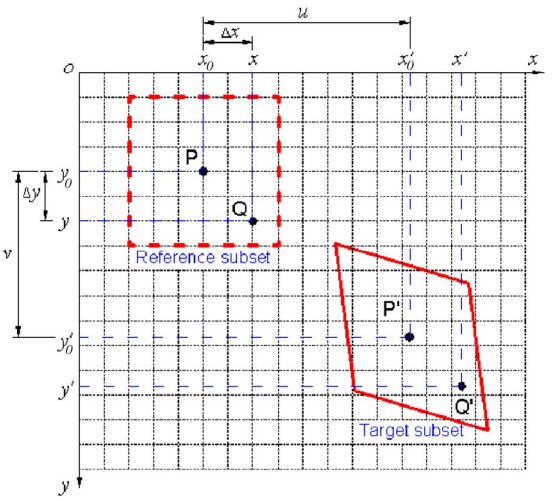

Fig. 1 Schematic diagram of reference and target (or deformed) subsets.

$\Delta x,\Delta y$ are the distance from the subset center P to point $Q(x,y)$, and u_x, u_y, v_x, and v_y are the displacement gradient components for the subset, as shown in Fig. 1.

2.3 *Correlation Function*

Let $f(x,y)$ and $g(x',y')$ represent the gray intensity distribution of the reference and target subsets respectively. To evaluate their similarity, a normalized least-square correlation function[12] is defined as

$$C_{f,g}(\vec{p}) = \sum_{x=-M}^{M}\sum_{y=-M}^{M}\left[\frac{f(x,y)-f_m}{\left\{\sum_{x=-M}^{M}\sum_{y=-M}^{M}[f(x,y)-f_m]^2\right\}^{1/2}} - \frac{g(x',y')-g_m}{\left\{\sum_{x=-M}^{M}\sum_{y=-M}^{M}[g(x',y')-g_m]^2\right\}^{1/2}}\right]^2, \tag{2}$$

where $f_m = 1/(2M+1)\Sigma_{x=-M}^{M}\Sigma_{y=-M}^{M} f(x,y)$, $g_m = 1/(2M+1)\Sigma_{x=-M}^{M}\Sigma_{y=-M}^{M} g(x',y')$ are the ensemble averages of reference and target subsets, respectively. $\vec{p}_{i=1,\cdots,6} = (u,u_x,u_y,v,v_x,v_y)^T$ denotes a vector with respect to six desired displacement mapping parameters.

It should be noted that the correlation function given in Eq. (2) is actually related to the commonly used zero-normalized cross-correlation function as demonstrated in Appendix A. Compared with the correlation function used in Refs. 4 and 5, the correlation function of Eq. (2) is more accurate to find the minimum coefficient due to an apparent sole and sharp peak existing in the correlation coefficient distribution. In addition, the correlation function shown in Eq. (2) exhibits robust anti-noise performances. As illustrated in Appendix B, it is insensitive to the linear transform of target subset gray intensity.

2.4 *Newton-Raphson Method*

The correlation function $C_{f,g}(\vec{p})$ defined in Eq. (2) is a nonlinear function of six unknown parameters [i.e., $\vec{p}_{i=1,\cdots,6}$

$=(u,u_x,u_y,v,v_x,v_y)^T]$ with range of $[0,+\infty)$. When the reference and target subsets get their maximum similarity, the minimum $C_{f,g}(\vec{p})$ is reached. In other words, the gradient of $C_{f,g}(\vec{p})$ must converge to zero, and then we have:

$$\nabla C_{f,g}(\vec{p}) = \left(\frac{\partial C}{\partial p_i}\right)_{i=1,\cdots,6} = -2\sum_{x=-M}^{M}\sum_{y=-M}^{M}\left[\left(\frac{f(x,y)-f_m}{\left\{\sum_{x=-M}^{M}\sum_{y=-M}^{M}[f(x,y)-f_m]^2\right\}^{1/2}} - \frac{g(x',y')-g_m}{\left\{\sum_{x=-M}^{M}\sum_{y=-M}^{M}[g(x',y')-g_m]^2\right\}^{1/2}}\right) \times \left\{\sum_{x=-M}^{M}\sum_{y=-M}^{M}[g(x',y')-g_m]^2\right\}^{-1/2} \cdot \frac{\partial g(x',y')}{\partial p_i}\right]_{i=1,\cdots,6} = 0. \quad (3)$$

The N-R method can be used to solve for roots of Eq. (3). The N-R equation can be correspondingly written as

$$\nabla C(\vec{p}) = \nabla C(\vec{p}_0) + \nabla\nabla C(\vec{p}_0)(\vec{p}-\vec{p}_0) = 0. \quad (4)$$

Rearranging Eq. (4), we get

$$\vec{p} = \vec{p}_0 - \frac{\nabla C(\vec{p}_0)}{\nabla\nabla C(\vec{p}_0)}, \quad (5)$$

where $\vec{p}_0$ is an initial guess of the solution, and $\vec{p}$ is the next iterative approximation solution of Eq. (5). $\nabla C(\vec{p}_0)$ is the first-order gradient of the correlation coefficient; $\nabla\nabla C(\vec{p}_0)$ is the second-order gradient of the correlation coefficient, also known as the Hessian matrix. According to the approach proposed by Vendroux and Knauss,[8] an approximation can be made to the Hessian matrix. Thus, it is can be expressed as

$$\nabla\nabla C_{f,g}(\vec{p}) = \left(\frac{\partial^2 C}{\partial p_i \partial p_j}\right)_{\substack{i=1,\cdots,6\\ j=1,\cdots,6}} \cong \frac{2}{\sum_{x=-M}^{M}\sum_{y=-M}^{M}[g(x',y')-g_m]^2} \times \sum_{x=-M}^{M}\sum_{y=-M}^{M}\left[\frac{\partial^2 g(x',y')}{\partial p_i \partial p_j}\right]_{\substack{i=1,\cdots,6\\ j=1,\cdots,6}}. \quad (6)$$

2.5 *Bicubic Spline Interpolation*

Because the coordinates of points in the deformed subset in Eq. (1) can assume subpixel values and no gray-level information is available between pixels in digital images, therefore, an interpolation scheme is needed in the realization of the N-R method. The selection of an interpolation scheme is considered as a key factor of the N-R method, because it directly affects the program's calculation accuracy and convergence character. In this study, a bicubic spline interpolation scheme[13] is implemented to determine the gray values and first-order gray gradients at subpixel locations as follows:

$$g(x,y) = \sum_{m=0}^{3}\sum_{n=0}^{3}\alpha_{mn}x^m y^n. \quad (7)$$

The unknown coefficients in Eq. (7) can be determined by the gray intensity of a interpolation area of given points (8×8 pixels in this study) and the continuity requirements. The N-R method using bicubic spline interpolation scheme shows high registration accuracy and good convergence character (commonly 2 to 6 iterations for each point in the following calculation), which is in good accordance with the results of Ref. 14.

2.6 *Convergence Conditions*

The convergence conditions were set to ensure that variations in displacements u and v were equal to or less than 10^{-4} pixels, and variations in displacement gradients were equal to or less than 5×10^{-6} (i.e., 5 $\mu\varepsilon$).

Both displacements and displacement gradients can be computed at each point of a virtual grid defined in the reference image using the above-mentioned N-R method. In addition, displacement gradients can also be obtained by differentiating the discrete displacements, as will be discussed in the following section.

3 Strain Calculation Using Two-Dimensional Savitzky-Golay Digital Differentiator

As we know, the relationship between the strain and displacement can be described as a numerical differentiation process in mathematical theory. In order to attain strain estimation, the most straightforward method is differentiating the estimated displacement fields. Unfortunately, the numerical differentiation is considered as an unstable and risky operation and should be undertaken with great caution because it can greatly amplify the noises, especially at high frequencies (i.e., the small fluctuations of the displacement estimates). Therefore, the resultant strains are untrustworthy if they are calculated by directly differentiating the estimated noisy displacements.

For convenience of explanation, consider the following example. If the registration error of displacement estimation is ±0.02 pixels and the grid step is 5 pixels, the error of resultant strain calculated by forward difference is $\Delta\varepsilon = 1/5\times(|\pm 0.02|+|\pm 0.02|)=8000\ u\varepsilon$, by central difference is $\Delta\varepsilon = 1/10\times(|\pm 0.02|+|\pm 0.02|)=4000\ u\varepsilon$. An error of that extent will probably hide the underlying strain information of the tested specimen and is unbearable in most cases.

3.1 *Strain Calculation*

Considering the unavoidable noises contained in the computed displacement field, the displacement field is locally fitted using the running least-squares method to calculate local strains. Since the noises can be largely removed in the process of local fitting, as a consequence, the accuracy of the calculated strains is greatly improved.

	x=-M	···	x=0	···	x=M
y=-M	u(-M,-M)	···	u(0,-M)	···	u(M,-M)
⋮	⋮	⋮	⋮	⋮	⋮
y=0	u(-M,0)	···	u(0,0)	···	u(M,0)
⋮	⋮	⋮	⋮	⋮	⋮
y=M	u(-M,M)	···	u(0,M)	···	u(M,M)

Fig. 2 Displacement data for local least-square fitting.

The basic idea behind the 2D SG digital differentiator is to fit a 2D polynomial to a local subregion of the displacement field centered at the current point O(0, 0), which contains uniformly distributed $(2M+1)\times(2M+1)$ data points, as illustrated in Fig. 2. The unknown polynomial coefficients can be computed using the least-square method. From the resulting polynomial coefficients, one can readily achieve partial derivatives of the center point O(0, 0). Then, the subregion moves to the next data point and repeats the above-mentioned calculation process.

To clearly describe the principle of the 2D SG digital differentiator, suppose that we want to fit a 2D polynomial of order one to the u,v displacement fields. The corresponding polynomials can be written as

$$u(x,y) = a_0 + a_1 x + a_2 y,$$

$$v(x,y) = b_0 + b_1 x + b_2 y, \tag{8}$$

where $x,y=-M:M, u(x,y), v(x,y)$ are the original displacements in the x and y directions at location (x,y) obtained by DIC. $a_{i=0,1,2}, b_{i=0,1,2}$ are the unknown polynomial coefficients. Therefore, the desired strains at the center point of the local subregion can be written as $\varepsilon_x=\partial u/\partial x=a_1$, $\varepsilon_y=\partial v/\partial y=b_2$, $\gamma_{xy}=(\partial u/\partial y)+(\partial v/\partial x)=a_2+b_1$.

Equation (8) can be rewritten in matrix form, and the least-square method can be used to solve the unknown polynomial coefficients. Therefore, the first equation of Eq. (8) can be expressed as

$$Xa = u \Rightarrow \begin{bmatrix} 1 & -M & -M \\ 1 & -M+1 & -M \\ \vdots & \vdots & \vdots \\ 1 & 0 & 0 \\ \vdots & \vdots & \vdots \\ 1 & M-1 & M \\ 1 & M & M \end{bmatrix} \begin{pmatrix} a_0 \\ a_1 \\ a_2 \end{pmatrix} = \begin{Bmatrix} u(-M,M) \\ u(-M+1,M) \\ \vdots \\ u(0,0) \\ \vdots \\ u(M-1,M) \\ u(M,M) \end{Bmatrix}. \tag{9}$$

From Eq. (9), we can get $a=(X^TX)^{-1}X^Tu$, where $(X^TX)^{-1}X^T$ is the pseudo-inverse matrix of X with a size of 3 rows and $(2M+1)\times(2M+1)$ columns and is independent of the displacement data. Each row of this pseudo-inverse matrix could be rearranged into a traditional filter of the same size of that of the subregion. The filter rearranged from the second row of $(X^TX)^{-1}X^T$ is of the form shown in Eq. (10):

$$\frac{3}{(2M+1)^2(M+1)M\times GS} \times \begin{bmatrix} -M & -(M-1) & \cdots & -1 & 0 & 1 & \cdots & M-1 & M \\ \vdots & \vdots & & \vdots & & \vdots & & \vdots & \vdots \\ -M & -(M-1) & \cdots & -1 & 0 & 1 & \cdots & M-1 & M \\ \vdots & \vdots & & \vdots & & \vdots & & \vdots & \vdots \\ -M & -(M-1) & \cdots & -1 & 0 & 1 & \cdots & M-1 & M \end{bmatrix}_{(2M+1)\times(2M+1)} \tag{10}$$

In Eq. (10), GS is the grid step. Equation (10) can be used to calculate $\partial u/\partial x=a_1$, $\partial v/\partial x=b_1$. The transpose of Eq. (10) is the corresponding 2D SG digital differentiator used for calculating $\partial u/\partial y, \partial v/\partial y$.

The calculation process of strains is performed by convolving the 2D SG digital differentiator with the displacement fields obtained by DIC. For example, to calculate $\varepsilon_x=\partial u/\partial x=a_1$, the calculation process can be represented mathematically as

$$\varepsilon_x(i,j) = \sum_{x=-M}^{M} \sum_{y=-M}^{M} h(x,y)u(i+x,j+y), \tag{11}$$

where $u(i,j)$ is the local displacement field centered at point (i,j), and $h(x,y)$ is the digital differentiator coefficients illustrated in Eq. (10).

Certainly, a polynomial of another order can also be used as fitting function. If the fitting function is of the form $f(x,y)=a_{00}+a_{10}x+a_{01}y+a_{20}x^2+a_{11}xy+a_{02}y^2$, a quadratic surface is employed to approximate the local subregion. Nevertheless, it can be easily found that the 2D SG digital differentiator deduced from a quadratic fitting surface will yield the same form as Eq. (10).

3.2 *Selection of Filter Size*

The selection of SG filter size is a key factor relating to the calculation result. Because a filter of large size contains more data points to calculate the local fitting, the influence of the noises (i.e., the small fluctuations of the displacement estimates) contained in the local displacement fields is weakened, and naturally, the smoothness of the resultant strain field will be improved. Generally speaking, two cases (i.e., homogeneous deformation and inhomogeneous deformation) should be created to discuss the influences of the filter size. In the case of a homogeneous deformation, large filter size will increase the accuracy of the strain estimation. However, in the case of an inhomogeneous deformation, a proper filter size should be carefully selected to get a balance between accuracy and smoothness. If the filter size is too large, the resultant strain field seems to be oversmoothed, and the strain values at neighboring positions tend to become equal.

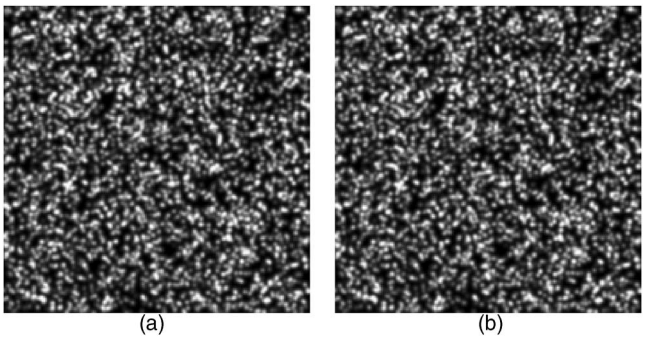

Fig. 3 Reference and deformed images of homogeneous deformation: (a) reference image and (b) deformed image.

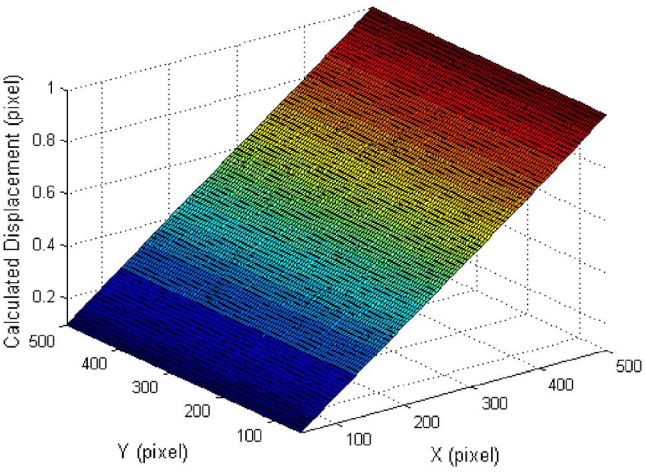

Fig. 4 The displacement field in the *x* direction obtained by the N-R method

4 Experimental Evaluation and Results

In the following study, two sets of test images representing homogeneous and inhomogeneous deformation cases, respectively, are employed to verify the effectiveness of the proposed technique. A subset of 51×51 pixels and grid step of 5 pixels were used in all computations demonstrated in the following.

4.1 *Homogeneous Deformation*

The first set of images was computer-simulated speckle images, which were generated according to the algorithm presented by Zhou et al.[5] The reference speckle image and the deformed speckle image are shown in Fig. 3(a) and 3(b), respectively. The preassigned homogeneous strain is 2000 $\mu\varepsilon$ in the horizontal direction of the image. The detailed features of the simulated speckle image are listed as follows: The size of simulated images is 576×576 pixels, the size of speckles is 4 pixels, the number of speckles is 4000 and the SNR is 20.

Figure 4 shows the displacement field in the horizontal direction obtained by the N-R method. It can be seen from Fig. 4 that the calculated displacement field agrees well with the preassigned linear distribution.

The strain field in the horizontal direction at 5,041 locations on a 71×71 grid directly obtained by the N-R method is exhibited in Fig. 5(a). By contrast, the corresponding strain field obtained by the convolution of 21×21 point 2D SG digital differentiator with the displacement field is exhibited in Fig. 5(b). As the actual strain is a constant value in the calculation area, we can clearly observe that the strain field obtained by the 2D SG digital differentiator is much better than that obtained directly by the N-R method.

Figure 6 shows the maximum, minimum, mean value, and standard deviation of strains obtained by various 2D SG digital differentiators from 3×3 to 21×21 points. It can be found in Fig. 6, although the mean strain values are all approximate, the preassigned one (the standard deviation of strain using larger filter size) decreases obviously.

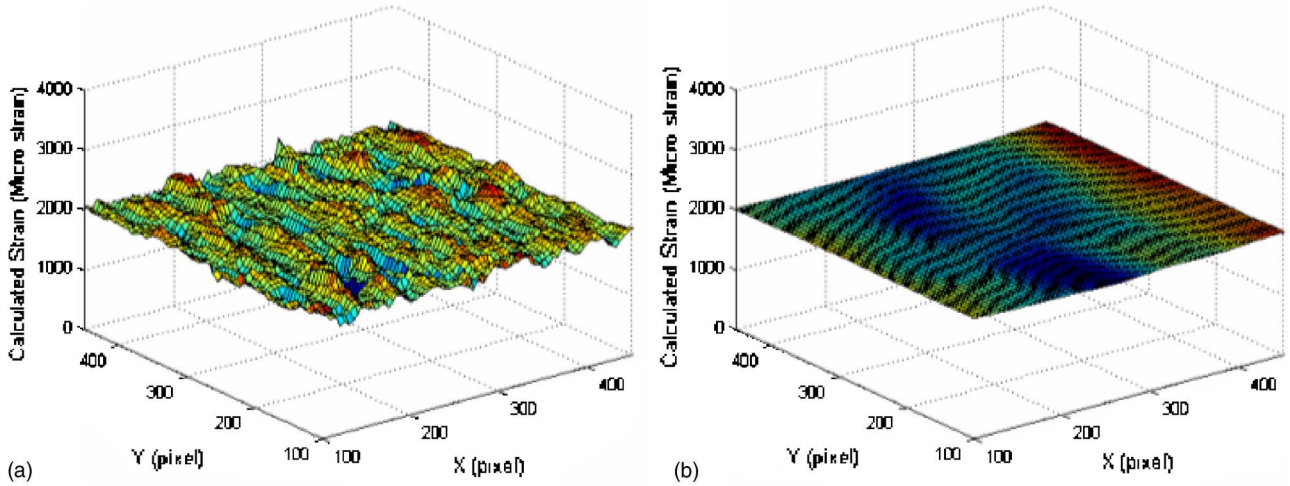

Fig. 5 The strain field obtained by (a) N-R method and (b) 21×21 point two-dimensional SG digital differentiator.

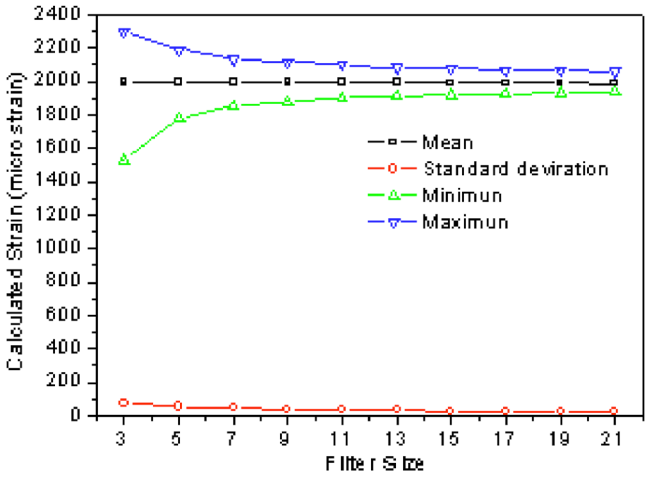

Fig. 6 The calculated strain of homogeneous deformation by various two-dimensional SG digital differentiators (unit: $u\varepsilon$).

This means that the accuracy of the strain measurement increases with the use of larger filter size in the case of homogeneous deformation.

4.2 *Inhomogeneous Deformation*

A three-point bending experiment was also performed on a material testing machine (WD1005, Changchun Kexin Co., Ltd, Changchun, China) to verify the proposed method as a case of inhomogeneous deformation. The specimen was made of PMMA material (Young's modulus $E=4.0$ Gpa and Poisson's ratio $v=0.35$ obtained from a uniaxial tensile experiment). Its geometry and loading condition are schematically shown in Fig. 7. The calculation area is on the center of the specimen [i.e., the blue rectangle area in the surface image shown as Fig. 7 and Fig. 8 (right) (color online only)]. The image with 768×576 resolution and 256 gray levels was captured by a CCD camera (Panasonic Wv-Bp330) with a magnification of 18.5 pixel/mm. The load was exerted by a round indenter and measured by the load sensor. A referenced image was obtained at 100 N and a deformed image was obtained at 700 N, as shown in Fig. 8.

The calculated u and v displacement fields at 5,661 locations on a 111×51 grid using the N-R method are shown in Fig. 9(a) and 9(b), respectively. We can see that the calculated displacement fields are reasonable and in agreement with the theory analysis of material mechanics. However, there apparently exist small fluctuations in the contour lines of estimated displacement fields, which can be attributed to the influence of unavoidable noises.

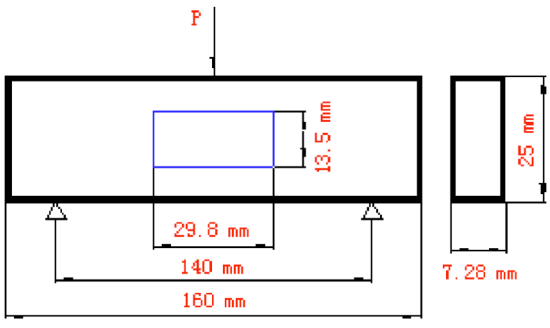

Fig. 7 Specimen geometry and loading condition of the three-point bending experiment.

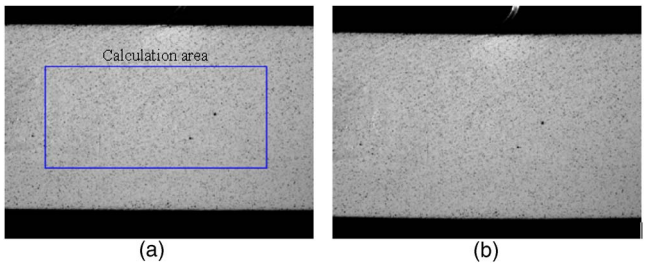

Fig. 8 The reference (a) and deformed (b) image of the three-point bending experiment.

The calculated εx and εy strain fields using the N-R method are shown in Fig. 10(a) and 10(b), repectively. It is obvious that the resulting strain distributions are very irregular, and no valuable information can be obtained from Fig. 10. This result also verifies the low accuracy of strains directly calculated using the N-R method.

The εx and εy strain fields obtained by the convolving 9×9, 15×15, and 21×21 point 2D SG digital differentiators, respectively, with the calculated displacement fields are shown in Fig. 11. We can observe from Fig. 11 that the strain fields are greatly improved compared with the strain fields directly obtained by the N-R method. With the increase of filter size, the smoothness and regularity of the strain fields are significantly improved.

An FEM analysis was also performed to obtain the ideal strain distribution of the specimen, and the corresponding results are shown in Fig. 12. By comparison, we can see that the calculated strain distributions by a 21×21 point 2D SG digital differentiator correspond well to theoretical calculations. Nevertheless, due to nonuniformity of actual specimen and the imperfection of the load conditions, the symmetry and magnitude of calculated strain distributions are not as perfect as those obtained from FEM analysis.

In this study, the grid step is chosen as fixed 5 pixels; 2D SG digital differentiators with filter size between 15×15 and 25×25 points is proper and recommended to use no matter what the deformation state is. However, it should be noted that the accuracy and smoothness of the resulting strain fields using the present technique rely heavily on the following two factors: the accuracy of the displacement fields obtained by DIC and the size of the SG digital differentiator used for calculating strain fields.

5 Conclusions

Unlike many research efforts that have been focused on how to improve the accuracy of displacement estimations, in this paper, we studied the technique for calculating strain in DIC. Based on the principle of local least-square fitting using 2D polynomials, 2D SG digital differentiators are deduced and used to differentiate the original noisy displacement fields obtained by DIC to get reasonable strain estimation. The calculation process can be easily implemented through the convolution operation. The calculated strain fields of two sets of test images of homogeneous and

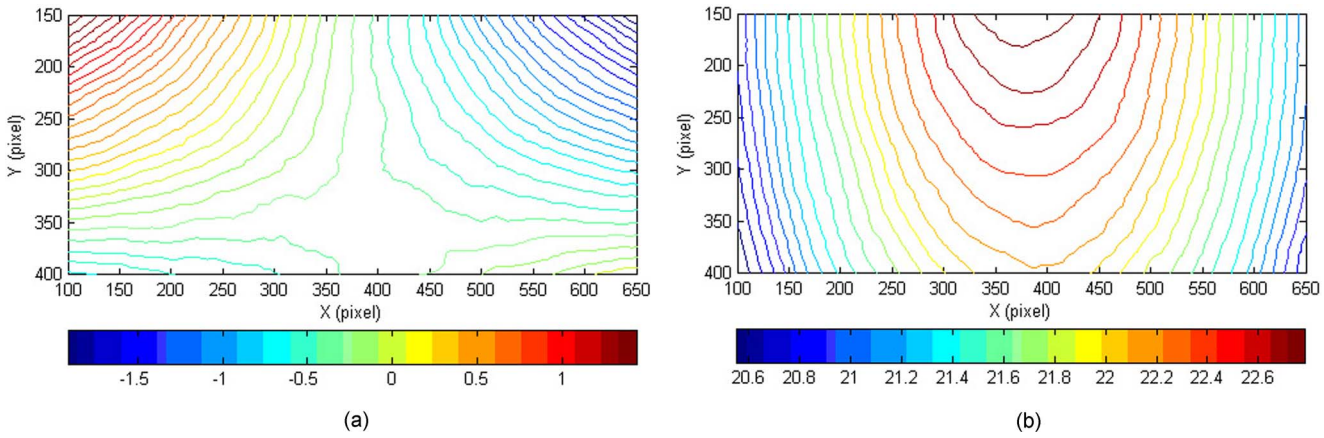

Fig. 9 The *u*, *v* displacement fields obtained by the N-R method.

inhomogeneous deformation, respectively, obviously demonstrate the validity of the proposed technique.

In comparison with the existing method involving smoothing the estimated displacement fields with penalty FEM first and subsequent differentiation to calculate strains, the advantages of the technique presented in this paper are given in the following three aspects:

- The underlying principle is quite clear and straightforward.
- The calculation process can be easily implemented by convolving the 2D SG digital differentiator with the obtained displacement field.
- The 2D SG digital differentiator can be arbitrary sizes easily adapted for different application cases.

In addition, this study also indicates that in order to obtain reasonable and accurate full-field strain estimation in DIC, the following two aspects are important and should be considered: the accuracy of displacement fields obtained by DIC and the size of the 2D SG digital differentiator used. In this study, a proper filter size is recommended to be chosen to achieve a good balance between resolution and smoothness in homogeneous deformation. Therefore, further study regarding the proposed technique is required to develop a 2D SG digital differentiator with self-adaptive size according to the noise levels contained in the local displacement fields.

Acknowledgments

This work is supported by the National Basic Research Program of China through Grant No. 2004CB619304; National Natural Science Foundation of China under Grant Nos. 10232030, 10121202, and 10472050; and the Specialized Research Fund for the Doctoral Program of Higher Education (20020003025).

Appendix A

The correlation function of Eq. (2) can be deduced from the commonly used zero-normalized cross-correlation function:

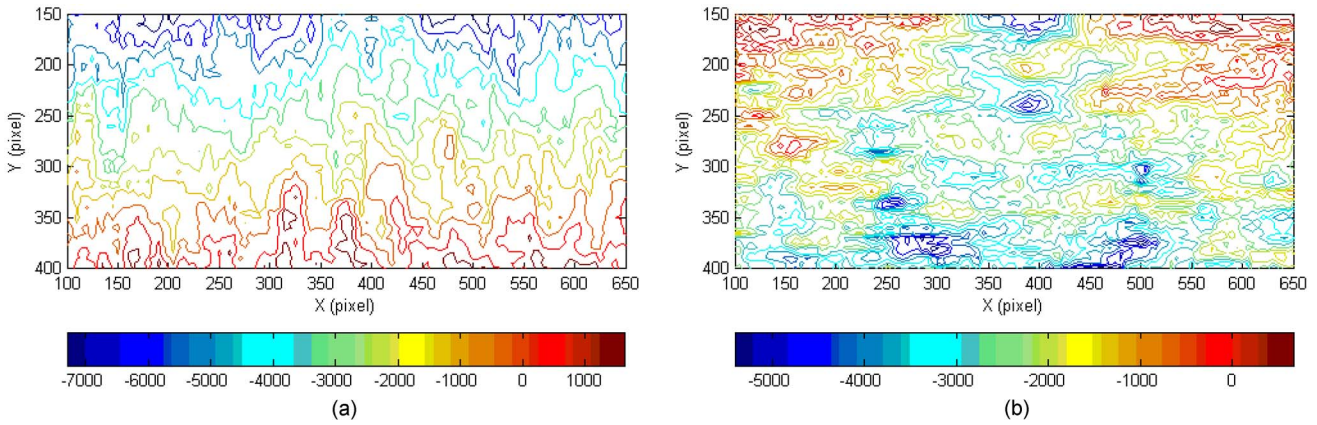

Fig. 10 The strain fields obtained by the N-R method (unit: $u\varepsilon$).

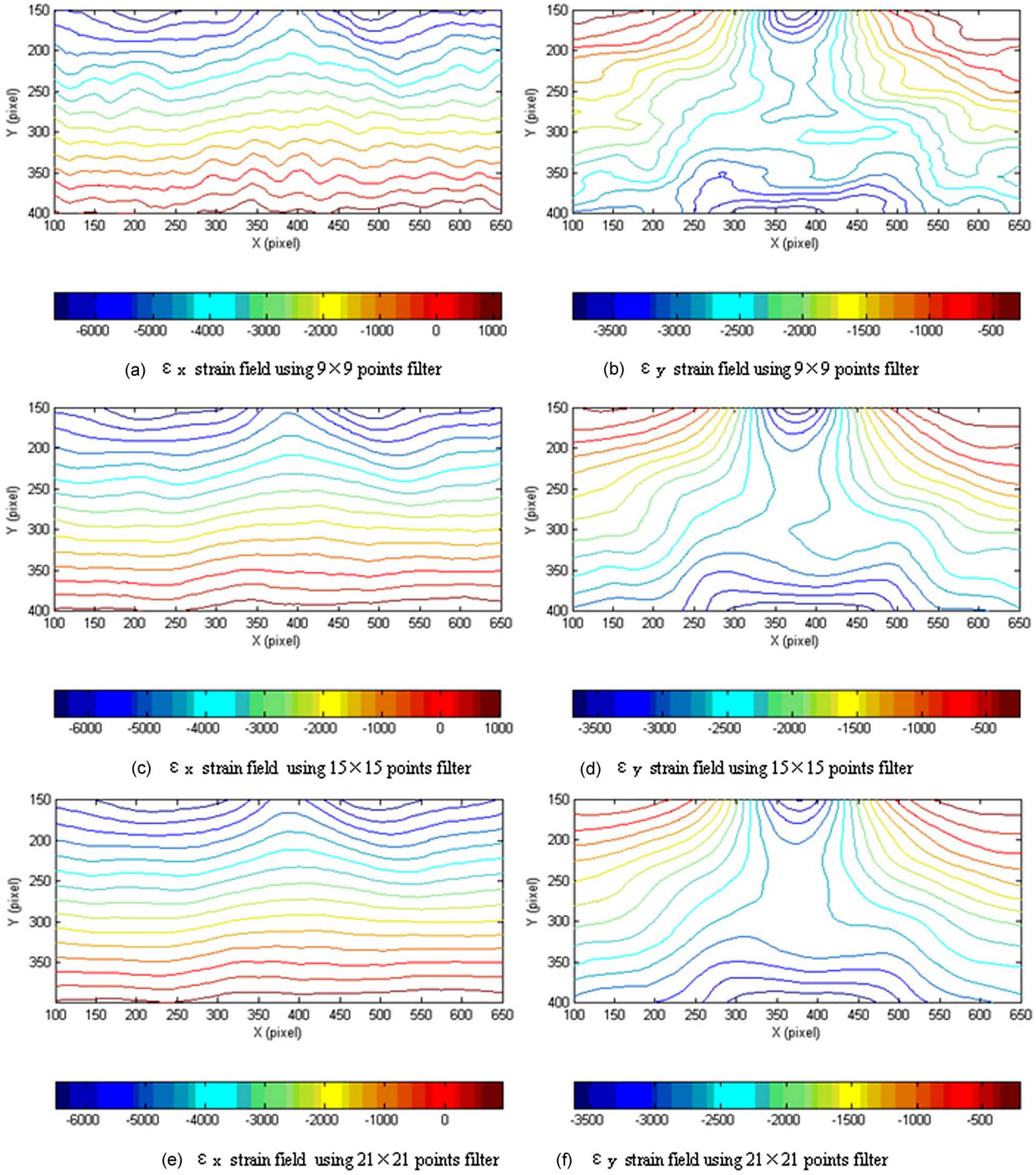

Fig. 11 The strain fields obtained by convolving various two-dimensional SG digital differentiators with the displacement fields of Fig. 9 (unit: $u\varepsilon$): (a) εx strain field using 9×9 point filter, (b) εy strain field using 9×9 point filter, (c) εx strain field using 15×15 point filter, (d) εy strain field using 15×15 point filter, (e) εx strain field using 21×21 point filter, and (f) εy strain field using 21×21 point filter.

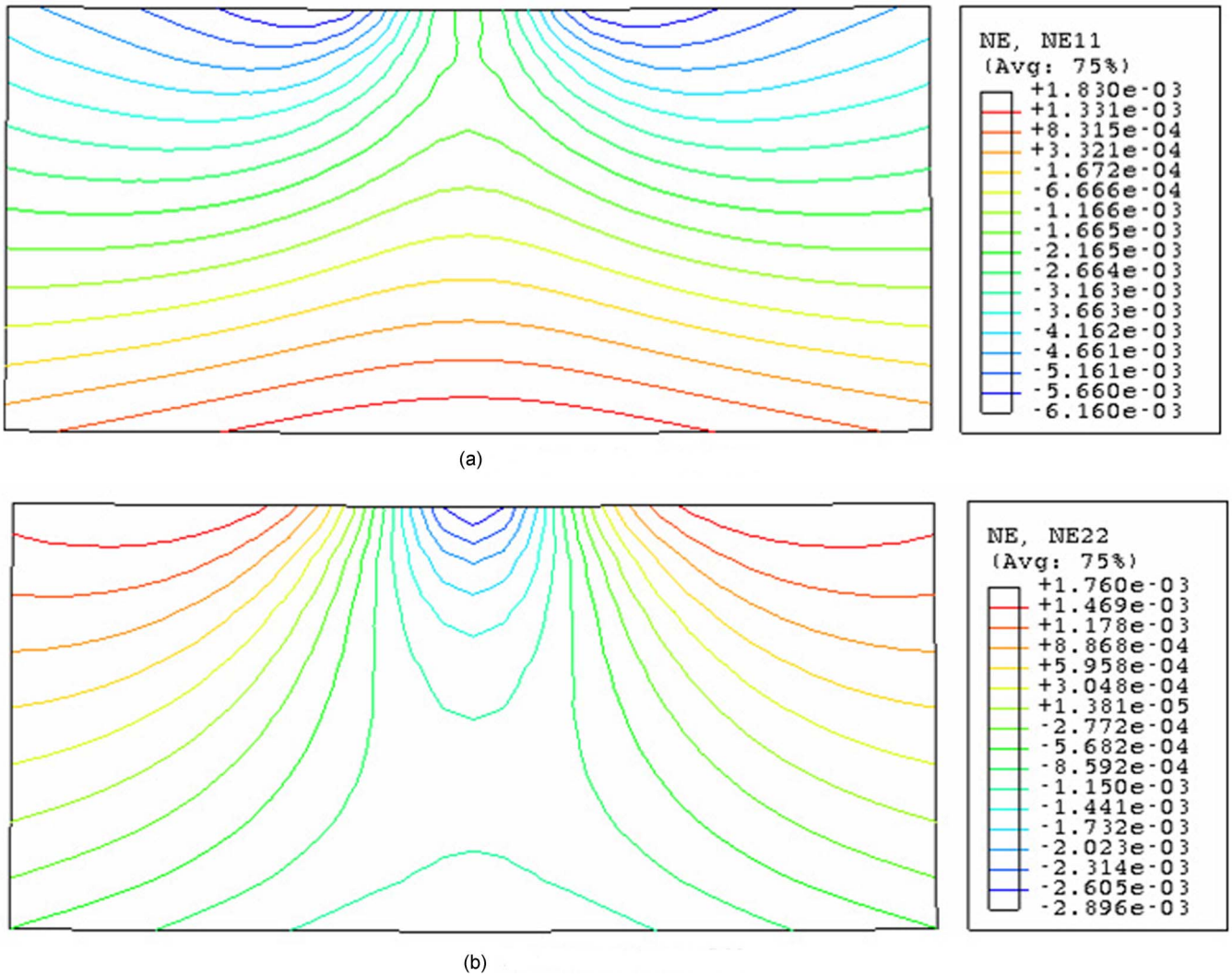

Fig. 12 The ideal εx (a) and εy (b) strain fields obtained by FEM analysis (unit: $u\varepsilon$).

$$
\begin{aligned}
C_{f,g}(\vec{p}) &= \sum_{x=-M}^{M}\sum_{y=-M}^{M}\left(\frac{f(x,y)-f_m}{\left\{\sum_{x=-M}^{M}\sum_{y=-M}^{M}[f(x,y)-f_m]^2\right\}^{1/2}}-\frac{g(x',y')-g_m}{\left\{\sum_{x=-M}^{M}\sum_{y=-M}^{M}[g(x',y')-g_m]^2\right\}^{1/2}}\right)^2 \\
&= \sum_{x=-M}^{M}\sum_{y=-M}^{M}\left[\left(\frac{f(x,y)-f_m}{\left\{\sum_{x=-M}^{M}\sum_{y=-M}^{M}[f(x,y)-f_m]^2\right\}^{1/2}}\right)^2+\left(\frac{g(x',y')-g_m}{\left\{\sum_{x=-M}^{M}\sum_{y=-M}^{M}[g(x',y')-g_m]^2\right\}^{1/2}}\right)^2\right. \\
&\quad \left.-2\frac{[f(x,y)-f_m]\times[g(x',y')-g_m]}{\left\{\sum_{x=-M}^{M}\sum_{y=-M}^{M}[f(x,y)-f_m]^2\right\}^{1/2}\left\{\sum_{x=-M}^{M}\sum_{y=-M}^{M}[g(x',y')-g_m]^2\right\}^{1/2}}\right] \\
&= 2\left(1-\frac{\sum_{x=-M}^{M}\sum_{y=-M}^{M}[f(x,y)-f_m]\times[g(x',y')-g_m]}{\left\{\sum_{x=-M}^{M}\sum_{y=-M}^{M}[f(x,y)-f_m]^2\right\}^{1/2}\left\{\sum_{x=-M}^{M}\sum_{y=-M}^{M}[g(x',y')-g_m]^2\right\}^{1/2}}\right). \qquad (12)
\end{aligned}
$$

Appendix B

If a linear transformation of the target subset gray intensity has been made according to function $g'(x',y')=a\times g(x',y')+b$, the correlation value computed using Eq. (2) is not changed.

$$
\begin{aligned}
C_{f,g'}(\vec{p}) &= \sum_{x=-M}^{M}\sum_{y=-M}^{M}\left(\frac{f(x,y)-f_m}{\left\{\sum_{x=-M}^{M}\sum_{y=-M}^{M}[f(x,y)-f_m]^2\right\}^{1/2}}\right. \\
&\quad \left.-\frac{ag(x',y')+b-ag_m-b}{\left\{\sum_{x=-M}^{M}\sum_{y=-M}^{M}[ag(x',y')+b-ag_m-b]^2\right\}^{1/2}}\right)^2 \\
&= \sum_{x=-M}^{M}\sum_{y=-M}^{M}\left(\frac{f(x,y)-f_m}{\left\{\sum_{x=-M}^{M}\sum_{y=-M}^{M}[f(x,y)-f_m]^2\right\}^{1/2}}\right. \\
&\quad \left.-\frac{ag(x',y')-ag_m}{\left\{\sum_{x=-M}^{M}\sum_{y=-M}^{M}[ag(x',y')-ag_m]^2\right\}^{1/2}}\right)^2 \\
&= C_{f,g}(\vec{p}) \qquad (13)
\end{aligned}
$$

References

1. W. H. Peters and W. F. Ranson, "Digital imaging techniques in experimental stress analysis," *Opt. Eng.* **21**(3), 427–431 (1982).
2. M. A. Sutton, S. R. McNeill, J. D. Helm, and Y. J. Chao, "Advances in two-dimensional and three-dimensional computer vision," in *Topics in Applied Physics*, P. K. Rastogi, Ed., vol. 77, pp. 323–372, Springer-Verlag (2000).
3. M. A. Sutton, S. R. McNeill, and J. Sengjang, "Effects of subpixel image restoration on digital correlation error estimate," *Opt. Eng.* **20**(10), 870–877 (1988).
4. H. A. Bruck, S. R. McNeil, M. A. Sutton, and W. H. Peters, "Digital image correlation using Newton-Raphson method of partial differential correction," *Exp. Mech.* **29**(3), 261–267 (1989).
5. P. Zhou and K. E. Goodson, "Subpixel displacement and deformation gradient measurement using digital image/speckle correlation," *Opt. Eng.* **40**(8), 1613–1620 (2001).
6. H. Jin and H. A. Bruck, "Theoretical development for pointwise digital image correlation," *Opt. Eng.* **44**(6), 1–14 (2005).
7. B. Pan, H.-M. Xie, B.-Q. Xu, and F.-L. Dai, "Performance of subpixel registration algorithms in digital image correlation," *Meas. Sci. Technol.* **17**(6), 1615–1621 (2006).
8. G. Vendroux and W. G. Knauss, "Submicron deformation field measurements: part 2 improved digital image correlation," *Exp. Mech.* **38**(2), 86–92 (1998).
9. H. Lu and P. D. Cary, "Deformation measurement by digital image correlation: implementation of a second-order displacement gradient," *Exp. Mech.* **40**(4), 393–400 (2000).
10. M. A. Sutton, J. L. Turner, H. A. Bruck, and T. A. Chao, "Full-field representation of discretely sampled surface deformation for displacement and strain analysis," *Exp. Mech.* **31**(2), 168–177 (1991).
11. A. Savitzky and M. J. E. Golay, "Smoothing and differentiation of data by simplified least squares procedures," *Anal. Chem.* **36**(8), 1627–1639 (1964).
12. W. Tong, "An evaluation of digital image correlation criteria for strain mapping applications," *Strain* **41**, 167–175 (2005).
13. W. H. Press, *C++ Numerical algorithms*, Publishing House of Electronics Industry, Beijing (2003).
14. H. W. Schreier, J. R. Braasch, and M. A. Sutton, "Systematic errors in digital image correlation caused by intensity interpolation," *Opt. Eng.* **39**(11), 2915–2921 (2000).

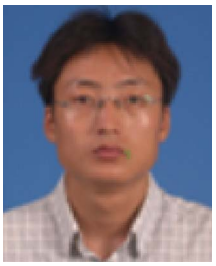

Bing Pan received his MS degree from the Department of Engineering Mechanics at the University of Science and Technology of China in 2004. He is currently pursuing his PhD degree in the Department of Engineering Mechanics at Tsinghua University. His research interests include digital image correlation and moiré method and their applications in experimental solid mechanics.

Huimin Xie is a full professor and the deputy head of the Key Lab of Failure Mechanics of the Ministry of Education of China at Tsinghua University. His research areas are in the development of new techniques and applications for solving challenging fundamental and industrial problems in the fields of experimental solid mechanics and applied optics. He is the associate editor-in-chief of the Chinese *Journal of Experimental Mechanics*, a steering committee member of the Asian Committee of Experimental Mechanics (ACEM), an editorial member of the *Journal of Optics and Lasers in Engineering* (Elsevier Science, UK) and *BSSM Journal of Strain* (Blackwell Publishing, UK). He has published more than ninety scientific papers in academic journals and proceedings of international conferences.

Zhiqiang Guo received his BS from Tsinghua University in Beijing in 2005. He is currently a graduate student in the Department of Engineering Mechanics at Tsinghua University.

Tao Hua received his BS from Tsinghua University in Beijing in 2004. He is currently a doctoral student in the Department of Engineering Mechanics at Tsinghua University.